Thick Target Bremsstrahlung Spectra for 1.00-, 1.25-, and 1.40-Mev Electrons*

WILLIAM MILLER, J. W. MOTZ, AND CARMEN CIALELLA†
Radiation Physics Laboratory, National Bureau of Standards, Washington, D. C.
(Received August 23, 1954)

The spectrum of radiation produced by 1.0-, 1.25-, and 1.40-Mev electrons incident on a thick tungsten target was measured at 0° and 90° with the incident beam by a method involving the magnetic analysis of Compton electrons. The effects of electron scattering and energy loss in the target preclude any simple interpretation of this data to yield a differential bremsstrahlung cross section. However, an estimate of the spectra to be expected at 0° and 90° was obtained by combining the Sauter expression for the bremsstrahlung cross section with the available information on electron scatter and energy loss in the target and backscatter from the target. The reliability of the estimate is limited because the Sauter formula was calculated by using the Born approximation, the electron scattering calculations are applicable to an infinite medium only, and the backscatter was estimated empirically from Bothe's experimental data which were obtained with lower energy electrons (370 kev). Furthermore electron energy straggling was neglected. Nevertheless, the predicted spectral shapes at 0° and 90° and the relative intensities at these two angles are in qualitative agreement with the measured values. The absolute magnitudes of the measured intensities at both angles are about a factor of two greater than the predicted values.

I. INTRODUCTION

EXPERIMENTAL investigations of the bremsstrahlung radiation from electrons in an energy range from 1.0 to 2.0 Mev have produced information about the angular distribution of the radiation from thick targets for different atomic numbers.[1] However information about the spectrum of photons produced by electrons in this energy range has been incomplete.[2]

This study was undertaken as part of a program to provide detailed information about the bremsstrahlung radiation for electrons with initial kinetic energies of the order of the electron rest energy. The present measurements[3] are concerned only with the radiation from the 2.8-mm tungsten target of the National Bureau of Standards 1.4-Mev accelerator.[4] The photon energy distribution for electrons with initial kinetic energies of 1.00, 1.25, and 1.40 Mev was measured with a magnetic Compton spectrometer.[5,6] The radiation was examined in directions parallel and perpendicular to the direction of the incident electron beam.

Previous estimates[1] of the spectrum to be expected from a thick target for electrons in this energy range, have depended on the theory developed by Kramers.[7] However, the validity of the Kramers' theory in the present case is limited: (a) the theory estimates the photon energy distribution integrated over all directions of the emitted photons, (b) the theory is nonrelativistic, (c) the effect of electron energy loss in the target is estimated on the basis of the Thomson-Whiddington law which is not valid for energies as high as those considered here, and (d) no account is taken of electron backscatter from the target. A more recent estimate of the spectrum to be expected from a thick target has been made by Wilson,[8] but his results also are in the form of an average over the direction of photon emission. In the present case, it is necessary to use the differential form (differential in photon energy and angle of photon emission) of the bremsstrahlung cross section, and then to estimate the modification produced in the radiation emitted from the target by electron energy loss and scattering in the target (including electron backscattering).

II. EXPERIMENTAL PROCEDURE

A schematic diagram of the experimental arrangement is shown in Fig. 1. Electrons with a given energy are focused on the thick tungsten target. Pinhole pictures indicate that the focal spot on the target has a diameter of approximately 5 mm. The target assembly shown in Fig. 1 is separated from the end of the vacuum chamber by a porcelain spacer. With this Faraday cup arrangement, target currents are measured with an accuracy of one percent. The electrostatic potential across the accelerator is determined with an accuracy of approximately one percent from measurements made with a high resistance voltmeter.[4]

The radiation passes from the target and the surrounding material shown in Fig. 1 to the lead collimator. The angle, ϕ, between the collimator-spectrometer axis and the direction of the incident electrons was adjusted for two separate values: $\phi=0°$ and $\phi=90°$. During a set of measurements, the radiation intensity was monitored by the integrated current output from an

* This work was supported by the U. S. Atomic Energy Commission.
† Present address: U. S. Geological Survey.
[1] Petrauskas, Van Atta, and Myers, Phys. Rev. **63**, 389 (1943); Buechner, Van de Graaff, Burrill, and Sperduto, Phys. Rev. **74**, 1348 (1948); Goldstein, Fano, and Wyckoff, J. Appl. Phys. **22**, 417 (1951).
[2] W. B. Lasich and L. Riddiford, J. Sci. Instr. **24**, 177 (1947); W. C. Miller and B. Waldman, Phys. Rev. **75**, 425 (1949).
[3] Other measurements involving the radiation from thin targets are now in progress.
[4] E. E. Charlton and H. S. Hubbard, Gen. Elec. Rev. **43**, 272 (1940).
[5] Motz, Miller, Wyckoff, Gibson, and Kirn, Rev. Sci. Instr. **24**, 929 (1953).
[6] Motz, Miller, and Wyckoff, Phys. Rev. **89**, 968 (1953).
[7] H. A. Kramers, Phil. Mag. **46**, 863 (1923).
[8] R. Wilson, Proc. Phys. Soc. (London) **A66**, 645 (1953).

ionization chamber placed in the photon beam at the back end of the spectrometer.

The collimated photon beam is incident on a beryllium foil, 0.96 cm long, 0.31 cm wide, and 0.0040 cm thick, and a magnetic analysis is made of the Compton electrons ejected from the foil into a small solid angle in the direction of the incident photon beam. A detailed description of the spectrometer and the method of data analysis have been given elsewhere.[5,6]

The spectrometer was calibrated with γ-ray sources of Co^{60} (1.17 Mev, 1.33 Mev), Cs^{137} (0.661 Mev) and Au^{198} (0.411 Mev).[9] The intensity of these sources was determined from measurements made with an extrapolation type ionization chamber.[10] The line shapes of the electron counting rate *versus* the magnetic field, which were obtained with the monoenergetic photons from these sources showed a resolution (full width at half maximum) of 4 percent.

III. RESULTS OF MEASUREMENTS

The spectra of the bremsstrahlung radiation emitted from the 2.8 mm tungsten target at angles of 0 degrees and 90 degrees to the incident electron direction are shown in Figs. 2 and 3 respectively, for tube voltages of 1000, 1250, and 1400 kilovolts. For each of the voltages, the measured target current was 0.5 ma. The values of the photon energy flux density, $P(k)$, are given at a position one meter from the target, and represent the photon energy distribution after filtration by the materials surrounding the target (see Fig. 1).

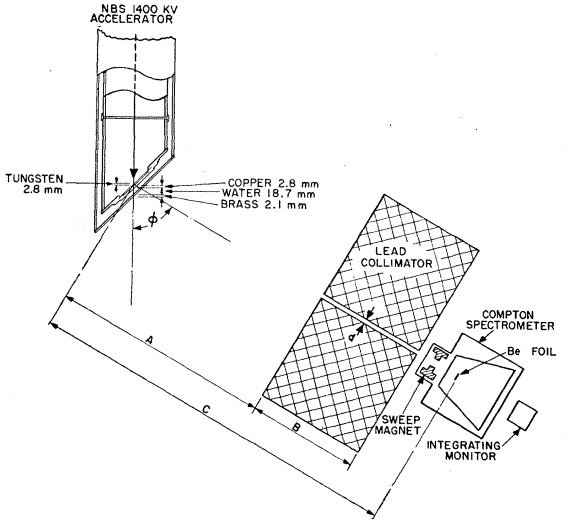

FIG. 1. Experimental arrangement for the bremsstrahlung measurements. Data were obtained for $\phi=0°$ and $\phi=90°$. The tungsten target was at an angle of 45° to the incident electron beam so that the filtration produced by the materials surrounding the target was the same in both the horizontal and vertical directions. For $\phi=0$ degrees; $A=31.1$ inches, $B=11.5$ inches, $C=54$ inches, and $d=0.308$ inch. For $\phi=90$ degrees; $A=34.5$ inches, $B=15$ inches, $C=58.5$ inches, and $d=0.541$ inch.

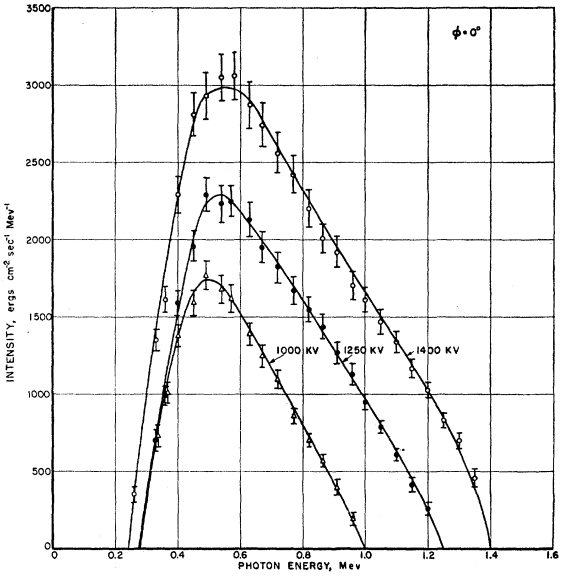

FIG. 2. Bremsstrahlung spectra at one meter from the target in the forward direction ($\phi=0°$), after radiation passes through materials surrounding target. The photon intensity was measured at a point 54 inches from the target (Fig. 1) and corrected for inverse square. The target current was 0.5 ma.

The dose rate which is produced at the position of the spectrometer foil by the photon energy flux density integrated over all photon energies for the spectra shown in Figs. 2 and 3, was computed by the use of true air absorption coefficients.[11] For comparison, the dose rate produced by the radiation at the foil position was measured with an extrapolation ionization chamber with $\frac{1}{4}$-inch Lucite walls. The measured dose rates were corrected for wall absorption and for the difference in stopping power of Lucite relative to air.[12] The dose rates determined by the above two methods are given in Table I, and show an agreement of approximately 10 percent.

IV. COMPARISON WITH THEORY

With a monoenergetic, monodirectional beam incident on a thick target, the spectral and angular distributions of the radiation leaving the target results from a superposition of several complex processes. These are:

(1) Radiation by monoenergetic, monodirectional electrons incident on a thin target; this is given by the differential bremsstrahlung cross section (i.e., differential in photon energy, photon angle, and electron energy).

(2) Electron penetration into a semi-infinite medium;

[9] *Nuclear Data*, National Bureau of Standards Circular 499 (U. S. Government Printing Office, Washington, D. C., 1950).
[10] G. Failla, Radiology **24**, 262 (1937).
[11] Gladys R. White (private communication).
[12] A 3 percent correction was applied for the difference in Lucite to air stopping power. See T. J. Thompson, University of California thesis, UCRL—1910, Aug. 11, 1952 (unpublished); and G. N. Whyte, Nucleonics **12**, No. 2, 19 (1954).

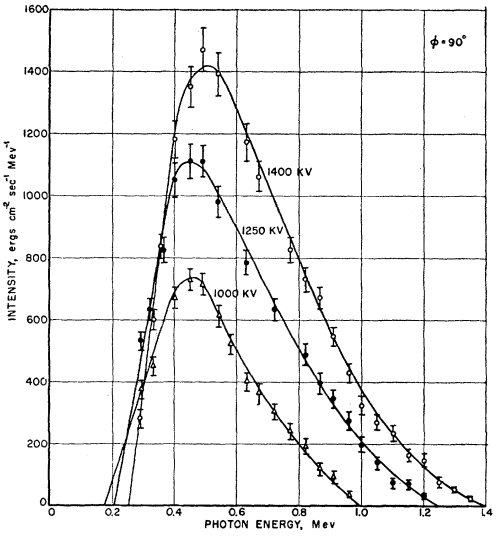

FIG. 3. Bremsstrahlung spectra at one meter from the target in the side direction ($\phi=90°$) after radiation passes through materials surrounding target. The photon intensity was measured at a point 58.5 inches from the target (Fig. 1) and corrected for inverse square. The target current was 0.5 ma.

this includes (a) angular dispersion of electron velocities, (b) backscatter out of the target, (c) energy loss.

(3) Absorption of photons in the target and surrounding materials.

Unfortunately, information on these individual processes is far from complete at present. The differential bremsstrahlung cross section has been computed in Born approximation by Sauter,[13] but the results are not strictly applicable here because of the high atomic number of the target material. Estimates have been made[14] of the error resulting from the use of the Born approximation in the nonrelativistic energy range, and Bethe and Maximon[15] have determined the correction which is applicable above 20 Mev. Interpolation between these corrections indicates that the Sauter formula underestimates the bremsstrahlung cross section for incident electrons with energies of approximately 1 Mev, but no quantitative estimate of the error is available. We shall use the Sauter formula to describe process (1) above, with these possible errors in mind.

With regard to process (2a), theories have been developed[16] to describe the angular distribution of electron velocities as a function of electron energy, for an initially monodirectional monoenergetic electron beam. However, these results apply to an infinite medium, and assume that the electron energy is a unique function of path-length (i.e., energy straggling is neglected). It is possible to get around the restriction to an infinite medium by considering the experimental results of Bothe[17] on backscattering. These show that (for the type of geometry in Fig. 1) very few electrons are backscattered until they have lost at least 10 percent of their energy. On the other hand, the electron scattering theories predict that in a heavy element like tungsten an initially monodirectional beam of electrons will have become almost completely isotropic by the time the electrons have lost about 10 percent of their energy.[18] This means that the angular diffusion process is essentially complete before a significant number of electrons get back to the surface. It seems plausible, then, that the electron scattering results obtained for an infinite medium will provide an approximate description for the semi-infinite medium.

The effect of electron backscatter (2b), is to cut down the number of electrons which can radiate. Bothe's[17] results indicate that well over half of the electrons incident at 45° on a high Z material like tungsten will eventually be backscattered. Furthermore, a large fraction of the backscattered electrons leave the target with at least 50 percent of their incident energy. It is apparent that backscatter causes a significant reduction in the total amount of radiation produced in the target. We shall account for backscattering by specifying that the number of electrons in the target decreases as the electron energy decreases.

The actual rate of decrease can be obtained from Bothe's data on the spectrum of backscattered electrons, with one modification. Electrons leaving the target are pointed away from the detector placed at 0° or 90° with the electron beam. Since the radiation from an electron is pretty well confined to the direction of the electron's motion, these electrons do not get radiation to the detectors just before leaving the target, and their loss is not felt immediately. One might say that loss of electrons by backscatter creates a "dip" in the angular distribution pattern, and this does not affect the amount of radiation reaching the detectors until the "dip" can diffuse around and decrease the number of electrons pointing towards the detectors. This diffusion is essentially completed in about the same time that the electrons lose about 10 percent of

TABLE I. Dose rates determined from spectrometer and ionization chamber measurements.

Tube voltage		Dose rate r min^{-1} ma^{-1} at one meter $\phi=90°$	$\phi=0°$
1400 kv	Ion. chamber	26±1	76±3
	Spectrometer	28±3	80±8
1250 kv	Ion. chamber	19±1	51±2
	Spectrometer	21±2	50±5
1000 kv	Ion. chamber	10±0.5	27±1
	Spectrometer	11±1	29±3

[13] F. Sauter, Ann. Physik **20**, 404 (1934).
[14] See W. Heitler, *The Quantum Theory of Radiation* (Oxford University Press, London, 1954), third edition, p. 246.
[15] H. A. Bethe and L. C. Maximon, Phys. Rev. **93**, 768 (1954).
[16] S. Goudsmit and J. L. Saunderson, Phys. Rev. **57**, 24 (1940); H. W. Lewis, Phys. Rev. **78**, 526 (1950).
[17] W. Bothe, Ann. Physik **6**, 44 (1949).
[18] This has been pointed out by U. Fano. See *Radiation Biology*, edited by A. Hollaender (McGraw-Hill Book Company, Inc., New York, 1954), Chap. I.

their energy. To allow for this, the distribution of backscattered electrons, as given by Bothe, has been scaled in energy. Thus, if Bothe's data indicate that a certain number of electrons are backscattered from the target with 80 percent of their initial energy, then in estimating the decrease in the number of electrons getting radiation to the detectors, these electrons are assumed to have been backscattered 10 percent later in energy, i.e., when they have $(0.9)\times 80$ percent, or 72 percent of their initial energy.

The main processes which cause the incident electrons to lose energy in the target are excitation and ionization of the target atoms (which results from collisions with atomic electrons) and radiation (which results mostly from collisions with nuclei). A comparison of the stopping power formula based on ionization and excitation[19] with the Sauter formula shows that a 1-Mev electron incident on a material with a high Z like tungsten will lose only a few percent of its energy by radiation. We shall make the simplifying assumption that the stopping power formula describes the energy loss of the electron, and that straggling may be neglected.

With regard to absorption of the radiated photons in the target and surrounding materials, it will be assumed that the photons of any energy are attenuated in a simple exponential manner. For the absorber thicknesses and Z values involved here it is sufficiently accurate to neglect "build-up" caused by Compton scattered photons ultimately reaching the detectors.

With the simplifying assumptions just outlined it is possible to carry through a calculation to estimate the spectrum of bremsstrahlung leaving the target at any angle with the direction of the incident beam of electrons. The kinetic energy of the incident electron beam will be taken as 1.4 Mev. In Fig. 4, the direction of the incident electron beam is taken as the forward direction, ϵ is the angle between electron velocity vector and forward direction, θ is the angle between photon and electron velocities, and φ is the angle between photon velocity and forward direction. If $I(k,\varphi)$ is defined as the intensity of photons per unit energy interval at energy k per steradian at angle φ, per incident electron,

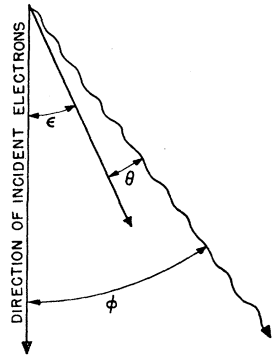

FIG. 4. Schematic representation of angles between photon direction (wavy line), direction of motion of an electron about to radiate, and the direction of the electron beam incident on the target.

[19] See W. Heitler, *The Quantum Theory of Radiation* (Oxford University Press, London, 1954), third edition, p. 386, Eq. (1).

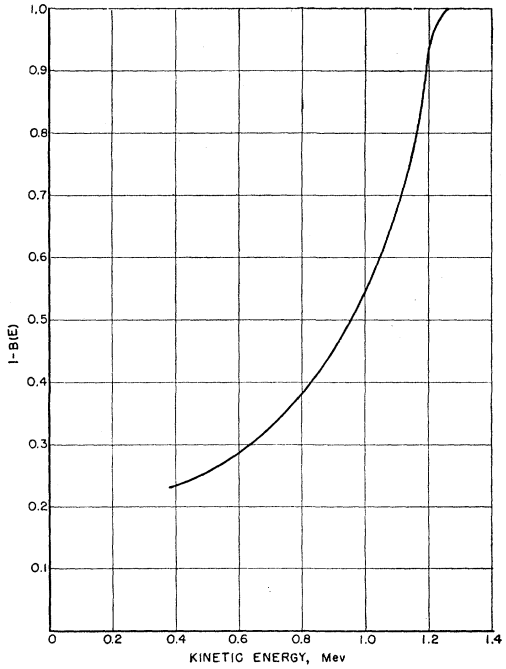

FIG. 5. The function $1-B(E)$.

then

$$I(k,\varphi)=N_A\int_{k+1}^{E_M}\int_0^{2\pi}\int_0^{\pi}N(E,\epsilon)\{1-B(E)\}\times k\sigma(E,k,\theta)\sin\epsilon d\epsilon d\psi\frac{ds}{dE}dE, \quad (1)$$

where N_A is the number of target atoms/cc, $B(E)$ corresponds to the fractional number of electrons of energy E which have been backscattered out of the target, $N(E,\epsilon)$ represents the angular distribution of the electron velocities as a function of electron energy, $\sigma(E,k,\theta)$ is the differential bremsstrahlung cross section, and ψ is the angle between the planes containing the angles ϵ and φ (Fig. 4), dE/ds is the stopping power, and E_M is the total energy of the incident electrons. The angle φ appears implicitly in Eq. (1) through the relationship $\cos\theta=\cos\epsilon\cos\varphi+\sin\epsilon\sin\varphi\cos\psi$. The kinetic energy of the incident electron has been set at 1.4 Mev for this calculation, so E_M is approximately $3.7mc^2$. The function $B(E)$ was empirically estimated from Bothe's data which was scaled in energy as described above. The resulting function $1-B(E)$ is shown in Fig. 5. Because the stopping power for electrons is a slowly varying function of energy at 1.4 Mev, dE/ds has been assigned a constant value. The value used is $43mc^2$/cm, and corresponds to the stopping power of a 1.4-Mev electron in tungsten, as calculated from the Bloch formula. The distributions $N(E,\epsilon)$ and $\sigma(E,k,\theta)$ have been approximated in the manner described above.

The angular distributions of the electrons and of the

bremsstrahlung cross sections are most conveniently expanded in Legendre polynomials:

$$N(E,\epsilon)=\frac{1}{4\pi}\sum_l f_l(E)P_l(\cos\epsilon), \tag{2}$$

$$\sigma(E,k,\theta)=\frac{\sigma(E,k)}{4\pi}\sum_m g_m(E,k)P_m(\cos\theta). \tag{3}$$

Since the intensity is being calculated per incident electron, $f_0(e)=1$. We also set $g_0(E)=1$, so that $\sigma(E,k)$ is the integral of $\sigma(E,k,\theta)$ over direction, and corresponds to the Bethe-Heitler cross section.

With the help of the addition theorem for Legendre polynomials, $P_m(\cos\theta)$ may be expressed in terms of $\cos\varphi$ and $\cos\epsilon$, and the angular integrations in Eq. (1) may then be carried out[20] to yield

$$I(k,\varphi)=\frac{N_A}{2}\int_{k+1}^{E_M}\{1-B(E)\}\frac{\sigma(E,k)}{4\pi}\sum_{l=0}^{\infty}\frac{2}{2l+1}\times f_l(E)g_l(E,k)P_l(\cos\varphi)\frac{ds}{dE}dE. \tag{4}$$

For electrons with energies in the range 0.4 to 1.4 Mev the Bethe-Heitler cross section may be approximated by

$$\sigma(E,k)\cong 11.5\left(1-\frac{k}{E-1}\right), \tag{5}$$

which is good to about 5 percent.

At this point it is easy to make a rough estimate of the average photon intensity spectrum to be expected, by assuming that all the electrons in the target are isotropic, and by neglecting backscatter effects. This means all f_l for $l>0$ are set equal to zero, as is $B(E)$. The spectrum calculated in this manner is shown in Fig. 6 as the dotted curve.

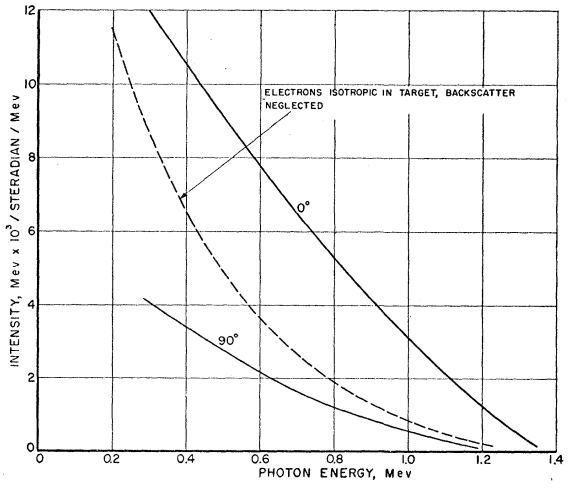

FIG. 6. Calculated spectral intensities per incident electron. (No adjustment has been made for photon absorption in the target and surrounding materials.)

[20] This integration is discussed in greater detail by O. Blunck, Ann. Physik 9, 25 (1951).

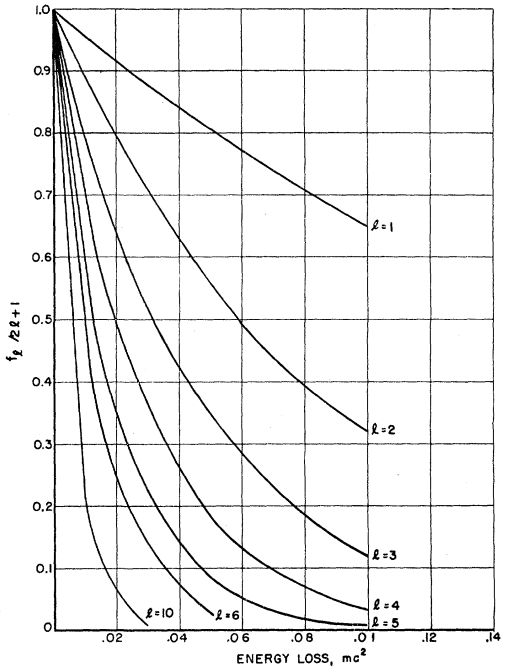

FIG. 7. Legendre coefficients for the angular distribution of electrons in tungsten. The incident electrons are monenergetic and have a kinetic energy of 1.4 Mev.

To determine the intensity and spectral dependence on angle, it is necessary to insert the values f_l and g_l into Eq. (4). The f_l have been determined by Lewis[16] who expanded the angular distribution of the electron velocity vectors in Legendre polynomials, and integrated the transport equation over the position variable. Using a relativistic, screened single scattering cross section calculated in Born approximation he obtained an expression for the Legendre coefficients of the form:

$$f_l=(2l+1)\exp\left(-\int_0^s K_l ds\right), \tag{6}$$

where s = total path length travelled by the electron, and

$$K_l\cong\frac{1}{2}\frac{2\pi N_A Z^2e^4}{p^2v^2}l(l+1)\left\{\ln\frac{4a_0^2p^2}{\hbar^2Z^{\frac{2}{3}}}+1-\sum_{m=1}^{l}m^{-1}\right\},$$

where a_0 is the Bohr radius. The f_l are readily expressed in terms of energy loss (if straggling is neglected) by inserting the stopping power formula into the integral over S. Figure 7 is a plot of f_l *versus* electron energy loss, for 1.4-Mev electrons in tungsten.

In principle, the g_l could be determined by integration over the analytical expression for the differential bremsstrahlung cross section. An alternative procedure is to actually plot the angular dependence of the

differential cross section, and numerically integrate to find the Legendre polynomial expansions for these curves. The latter procedure is much simpler than the analytic method because of the complexity of the differential cross-section formula. The graphical method was actually used to determine the g_l, and although the numerical work was only carried to an accuracy of about 5 percent, this is not inconsistent with the uncertainty in the backscatter estimate. Figure 8 is a representation of the values obtained for the g_l for selected values of electron and photon energies. Interpolations were carried out to supply the values necessary to complete the integrations and sums in Eq. (4). The distributions thus obtained were multiplied by photon energy to yield the spectral intensity distributions at

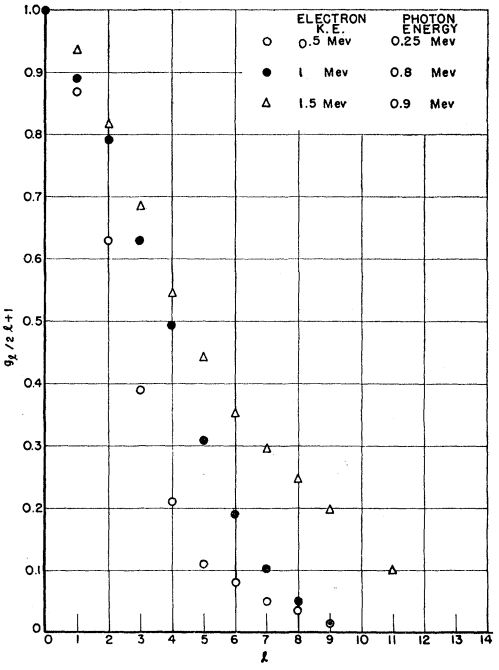

FIG. 8. Legendre coefficients for the angular distribution of bremsstrahlung, for selected values of electron and photon energies.

0° and 90°. These are indicated by the solid lines of Fig. 6.

The computed spectra at 0° and 90°, for 1.4-Mev electrons, shown in Fig. 6 must be modified to account for attenuation in the target and surrounding media, before they can be compared with measured spectra. In computing the attenuation, the thickness of the target was estimated to be 2.8 mm on the basis of a radiograph, and the absorbing thickness was taken as 2.4 mm to allow for the fact that the x-rays are produced at some small depth in the target. The absorption curve, Fig. 9, was constructed from the narrow beam absorption data of White,[11] and absorber thicknesses corresponding to dimensions shown in Fig. 1. The 1.4-Mev spectra of Fig. 6 multiplied by the attenuation curve of Fig. 9, are indicated by the solid curves in

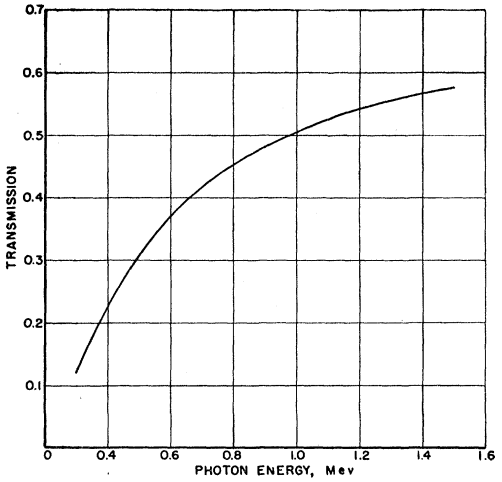

FIG. 9. Estimated absorption in the target and surrounding materials. The effective absorbing thickness of the target was assumed to be 2.4 mm. The thicknesses of the additional absorbing materials are given in Fig. 1.

Fig. 10. For comparison, the observed spectra for 1.4-Mev electrons at 0° and 90° (Figs. 2 and 3) have also been plotted in Fig. 10. The intensity scale per incident electron is in units of 2.1×10^{-3} (Mev/Mev) per steradian for the experimental data, and 10^{-3} (Mev/Mev) per steradian for the computed curves. These scale factors were chosen so that the computed and experimental data at 0° would agree at their peak values.

A comparison of the measured and computed curves in Fig. 10 shows that the energy distributions and the relative intensities of the radiation at 0° and 90° are in qualitative agreement. However, the absolute in-

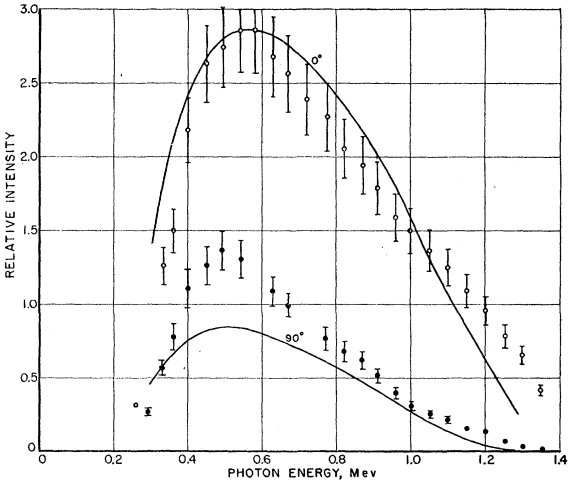

FIG. 10. Computed and experimentally determined relative spectral intensities at 0° and 90°. The solid curves were obtained by applying the transmission curve (Fig. 9) to the computed spectra (Fig. 6). The experimental points correspond to the 1400-kev data on Figs. 2 and 3. To obtain absolute spectral intensities, in Mev per steradian per Mev per incident electron, the ordinate should be multiplied by 10^{-3} for the computed curves, and by 2.1×10^{-3} for the experimental points.

tensities indicated by the measured curves are about a factor of two greater than the values given by the theoretical curves. There is earlier evidence[21] indicating that use of the Born approximation yields an underestimate of the bremsstrahlung cross section for electrons in this energy range. A detailed examination of this question by the use of thin targets is now in progress.[22] With regard to the angular distribution of the radiation, it is interesting to note the extent to which the angular diffusion of the electrons in the target smear the radiation pattern. This smearing is evident when one compares the intensity ratio at 0° and 90° for thin and thick targets; the Sauter formula gives an intensity ratio of about 200, while the thick target results give an intensity ratio of about three.

The writers wish to thank Dr. H. O. Wyckoff for his advice during the course of this work, and F. H. Attix for his help in carrying out the ionization chamber measurements.

[21] H. Klarmann and W. Bothe, Z. Physik **101**, 489 (1936).

[22] A preliminary report on these thin target measurements by Motz and Miller, to be published, indicates a similar disagreement between theory and experiment for 1-Mev electrons.

PHYSICAL REVIEW VOLUME 96, NUMBER 5 DECEMBER 1, 1954

Orbital Electron Capture in the Heaviest Elements*†

R. W. Hoff and S. G. Thompson
Radiation Laboratory and Department of Chemistry, University of California, Berkeley, California

(Received August 20, 1954)

Logft values have been calculated for 30 orbital electron capture isotopes in the heaviest elements ($Z=89$–97). The average values of logft products for negative beta particle transitions have been used to classify the electron capture transitions studied as to forbiddenness. A logarithmic plot of the electron capture partial half-life *versus* neutrino energy has been made for both the allowed and forbidden species. These diagrams can be used in the prediction of electron capture half-lives where one has some insight into the amount of decay energy available.

THE orbital electron capture process can be studied with particular effectiveness in the heaviest elements since decay energies may be calculated from closed decay cycles. Because of inherent experimental difficulties, only a limited number of decay energies for electron capture have been determined either from continuous gamma ray spectra or from competing positron emission of known energy. In the region of atomic number greater than 82, Seaborg and co-workers[1] have used closed decay cycles to calculate decay energies for a large number of electron capture isotopes. Thompson[2] and Feather,[3] in earlier studies of electron capture, have plotted half-life as a function of energy for a number of electron capture nuclides in the heavy region. From a consideration of this type of diagram, the nuclides were classified according to the allowed or forbidden nature of the transition. However, these correlations were limited by a lack of experimental data. Major and Biedenharn[4] have extended these studies to lighter nuclei wherever half-life, branching ratio, and transition energy are known. They conclude that the scatter of the data on such a diagram does not permit differentiation as to degrees of forbiddenness.

A more fundamental indication, the ft value, has been used in the present work to determine the nature of electron capture transitions. The appropriate value of the function f of energy and atomic number was calculated considering allowed electron capture from the K and L shells only using the formulas given by Marshak.[5] This value was multiplied by the electron capture half-life to form the ft product. Table I lists logft values for nuclides whose electron capture decay schemes are known or can be inferred from the negative beta particle or alpha decay of an isotope to the same daughter nucleus. In certain cases where relative intensities of gamma and x-rays are not known, it has been assumed that the majority of the electron capture decay proceeds to the excited levels in the daughter nuclei. Logft values calculated for these transitions will not be affected greatly by a certain amount of branching decay to the ground states of the daughter nuclei.

Another group of nuclides exists for which decay schemes are not known. Logft values have been calculated for these isotopes under the assumption of ground state transitions. Obviously this assumption is not realistic, but it is the only method of treating the data

* Most of the material in this article is presented in greater detail in the Ph.D. thesis, R. W. Hoff, University of California Radiation Laboratory Declassified Document UCRL-2325, 1954 (unpublished).

† This work was performed under the auspices of the U. S. Atomic Energy Commission.

[1] Seaborg, Glass, and Thompson (to be published); R. A. Glass, Ph.D. thesis, University of California Radiation Laboratory Unclassified Document UCRL-2560, April 1954 (unpublished).

[2] S. G. Thompson, Phys. Rev. **76**, 319 (1949).

[3] N. Feather, Proc. Roy. Soc. (London) **A63**, 242 (1952).

[4] J. K. Major and L. C. Biedenharn, Phys. Rev. **94**, 779 (1954).

[5] R. E. Marshak, Phys. Rev. **61**, 431 (1942).